

17. Heflin, J. R.; Wong, K. Y.; Zamani-Khamiri, O.; Garito, A. F. *Phys. Rev. B* 1988, 38, 1573.
 18. de Melo, C. P.; Silbey, R. *Chem. Phys. Lett.* 1987, 140, 537.
 19. de Melo, C. P.; Silbey, R. *J. Chem. Phys.* 1988, 88, 2558.
 20. de Melo, C. P.; Silbey, R. *J. Chem. Phys.* 1988, 88, 2567.

Synthesis, Properties and Structures of Discotic Liquid Crystalline Porphyrins

Kwang-Sup Lee*, Jong-Il Shin, Young-Sup Shim,
 Young Key Shim†, Seiji Isoda‡, and Jung-Il Jin*

Department of Macromolecular Science, Han Nam
 University, Taejon 300-791, Korea

†Pharmaceutical Division, Korea Research Institute for
 Chemical Technology, Taejon 305-340, Korea

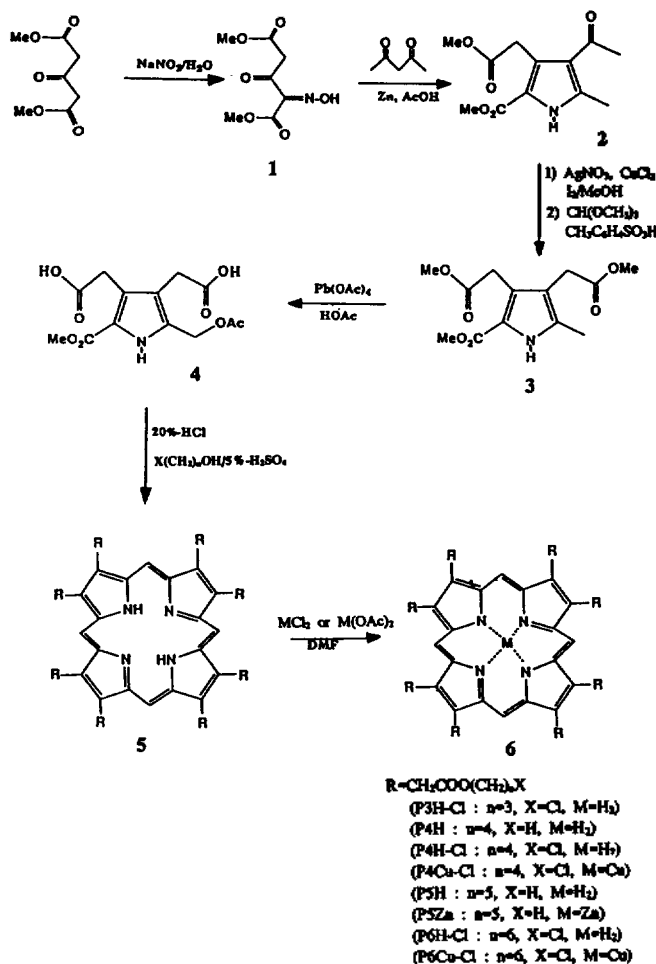
‡Institute for Chemical Research, Kyoto University,
 Uji, Kyoto 600, Japan

*Department of Chemistry, Korea University,
 Seoul 136-701, Korea

Received June 14, 1994

In recent years, discotic liquid crystals composed of flat rigid aromatic cores and flexible side chains have intensively been investigated for the applications as optical sensors, one-dimensional conductors, electrocatalysts etc.¹⁻⁵ We have synthesized several discotic liquid crystalline porphyrin derivatives having eight long alkylester chains. They contain two different central metals and eight side chains with various lengths of alkylgroups. This enables us to have the knowledge of transition temperatures from the crystalline phase to mesophase as well as structural changes between crystalline phase and mesophase.

Scheme 1 depicts the route to synthesize liquid crystalline porphyrin derivatives. By the reaction of β -ketoester with aq. sodium nitrite, dimethyl-1,3-acetonedicarboxylate oxime 1 was obtained. Methyl-3-acetyl-5-(methoxycarbonyl)-2-methylpyrrole-4-acetate 2 was prepared from 2,4-pentanedione and oxime derivative 1 in 49% yield by Knorr method for pyrrole synthesis.⁶ After iodination of the acetyl terminal group of pyrrole 2, the resulting iodoacetyl pyrrole was reacted with trimethyl orthoformate/p-toluene sulfonic acid to get the dimethyl 5-(methoxycarbonyl)-2-methylpyrrole-3,4-diacetate 3 in 82% yield.⁶ Continually, by the oxidation of compound 3 using lead tetracetate in acetic anhydride/acetic acid, dimethyl 5-(methoxycarbonyl)-2-(acetoxymethyl) pyrrole-3,4-diacetate 4 was obtained in nearly quantitative yield by a standard procedure.⁷ Thereafter reactions were performed in one reactor without isolation of intermediates. In this reaction, the α -ester group of compound 4 was hydrolyzed firstly and then the ring-closure reaction for porphyrins was done using 5% sulfuric acid with alcohol.⁸ In this step, alkyl ester groups with different chain lengths were introduced



Scheme 1.

using appropriate alcohols. Finally the metalloporphyrins were obtained by refluxing the corresponding porphyrins using metal acetate or chloride in dimethylformamide.⁹

Reaction intermediates and final products were characterized by ¹H NMR spectroscopy. Obtained structures were matched with corresponding compounds. As representatives of this series, signals around -3.6 ppm and 10.3 ppm in ¹H NMR for metal-free butylester-attached porphyrin (P4H)¹⁰ and chlorobutylester-attached porphyrin (P4H-Cl),¹¹ indicate -NH and meso-CH of aromatic porphyrins, respectively. The strong absorption peak, so called Soret band, at 405 nm in a UV spectrum of P4H which indicates porphyrin ring formation was also observed. When this porphyrin have no metal in the cavity, four weak absorption peaks appear at higher wavelength at 475, 523, 580 and 637 nm along with strong Soret band. However, in the case of metal complexation in the cavity, only two absorption peaks appeared. Such spectral features are already well known in porphyrin chemistry.^{8,12} For other porphyrin derivatives similar spectral features were also observed.

The research on the resulting porphyrins focused on the possibility to control liquid crystalline transition temperature by insertion of different metals in the porphyrin cavity, and by substitution of heavy atoms in the side chain terminal as well as by attaching different side chain lengths. The answers to such objectives can be given in differential scanning

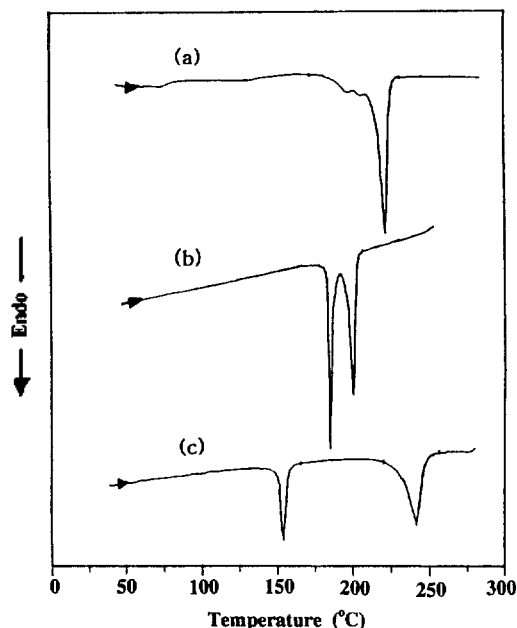


Figure 1. DSC curves obtained from first heating scan of porphyrins; (a) P4H, (b) P4H-Cl and (c) 4Cu-Cl.

Table 1. Thermal Transition Data of Liquid Crystalline Porphyrin Derivatives^a

Samples	T_D^b (°C)	T_I (°C)
P3H-Cl	250, 262	275
P4H	180, 200	225
P4H-Cl	180	200
P4Cu-Cl	155	242
P5H	135	200
P5Zn	138	221
P6H-Cl	?	146
P6Cu-Cl	155	178

^a Transition temperatures were detected from first heating scan by DSC (heating rate 10 °C/min). ^b Discotic mesophase temperature. ^c Isotropic melting temperature.

calorimetry (DSC) through heating process. Figure 1 shows typical DSC thermograms for P4H, P4H-Cl and P4-Cu-Cl as the representatives. In the case of P4H which has no metal in the cavity and no heavy atom in side chain terminal, the porphyrin does not show discrete enthalpy change in liquid crystalline phase. However, the heavy atom in the side chain terminal exists, liquid crystalline endothermic peak at 180 °C becomes stronger, and when two factors, *i.e.*, metal and heavy atom are involved, a broad liquid crystalline range of 89 °C ($T_D=155$ °C, $T_I=242$ °C) is observed. Such results are very helpful when we consider the use of porphyrin as opto-electronic device materials.

Exothermic peaks of all porphyrin derivatives obtained in this work are summarized Table 1. The porphyrins with longer side chains tend to melt at a lower temperature; P3H at 275 °C, P4H-Cl at 200 °C and P6H-Cl at 146 °C, respectively.

Table 2. Structural Parameters of Porphyrin Derivatives^a

Porphyrins	Crystal	Discotic Liquid Crystal Phase	Melt
P5H, P5Zn	Monoclinic	Pseudo-hexagonal	
	$a=1.86$ nm	$a=2.32$ nm	1.93 nm
	$b=2.27$ nm	$c=0.46$ nm	0.47 nm
	$c=0.49$ nm		
	$\alpha=114^\circ$		
P4Cu-Cl	triclinic	pseudo-hexagonal	
	$a=1.93$ nm	$a=2.25$ nm	1.94 nm
	$b=2.27$ nm	$b=0.46$ nm	0.47 nm
	$c=0.49$ nm		
	$\alpha=90^\circ$		
	$\beta=114^\circ$		
	$\gamma=97^\circ$		
P6Cu-Cl	triclinic	pseudo-hexagonal	
	$a=1.93$ nm	$a=2.56$ nm	2.56 nm
	$b=2.61$ nm	$c=0.46$ nm	0.47 nm
	$c=0.49$ nm		
	$\alpha=90^\circ$		
	$\beta=114^\circ$		
	$\gamma=97^\circ$		

^a The data were obtained from X-ray scattering and electron diffraction experiments^{13,14}

However, mesophase transition temperatures seem to depend not on the side chain lengths (P4Cu-Cl at 155 °C and P6Cu-Cl at 155 °C), but on the kind of metal ligands (P5H at 135 °C and P5Zn at 138 °C) and the end atoms in the side chains (P4H at 180 °C and P4H-Cl at 180 °C). All porphyrin derivatives when examined under polarizing microscopy exhibit leaf-like textures indicative of discotic phases.

The structure of some porphyrin samples was investigated by X-ray¹³ and electron diffraction.¹⁴ The structural parameters are listed in Table 2. P5H and P5Zn have almost the same monoclinic structure with $a=1.86$ nm, $b=2.27$ nm, $c=0.49$ nm and $\beta=114^\circ$ in crystalline phase at room temperature. The b-axis dimension of P4Cu-Cl shows the same value with P5H, which may be resulted from the fact that they have the same side chain lengths because of the same Van der Waals radii for methyl groups and chlorine atoms. P4Cu-Cl and P6Cu-Cl have the triclinic structure with different b-axis dimensions depending on their side chain lengths. The c-dimensions are the same in all porphyrin derivatives. At higher temperatures they transform into discotic phase with pseudo-hexagonal symmetry with $a=2.25\sim 2.56$ nm and $c=0.46$ nm. Above isotropic melting temperatures, the diffraction patterns show only broad peaks at the d -spacings of 1.93–2.56 nm and 0.47 nm. This may correspond to the interplanar spacings between planar porphyrin moieties and those between the side-by-side packing among the molecular columns, respectively.

Acknowledgment. This research was supported by a grant from the Basic Science Institute Program, Ministry of Education of Korea.

References

1. Belarbi, Z.; Sirlin, C.; Simon, J.; Andre, J.-J. *J. Phys. Chem.* **1989**, *93*, 8105.
2. Piechocki, C.; Simon, J.; Skoulios, A.; Guillon, D.; Weber, P. *J. Am. Chem. Soc.* **1982**, *104*, 5245.
3. Gregg, B. A.; Fox, M. A.; Bard, A. J. *J. Am. Chem. Soc.* **1989**, *111*, 3024.
4. van Nostrum, C. F.; Nolte, R. J. M. *Polym. Preprints* **1993**, *34*, 164.
5. Gregg, B. A.; Fox, M. A.; Bard, A. J. *J. Chem. Soc., Chem Commun.* **1987**, 1134.
6. Franck, B.; Wegner, C.; Bringmann, G.; Fels, G. *Liebigs Ann. Chem.* **1980**, 253.
7. Siedel, W.; Winkles, F. *Liebigs Ann. Chem.* **1943**, 554, 162.
8. Franck, B. *Angew. Chem., Int. Ed. Engl.* **1982**, *21*, 343.
9. Adler, A.-D.; Longo, F. R.; Kampas, F.; Kim, J. *J. Inorg. Nucl. Chem.* **1970**, *32*, 2443.
10. Physical, spectral and elemental analysis data of P4H: mp. 225°C ¹H NMR (CDCl₃), δ (ppm) -3.62 (b, 2H, NH), 0.74 (t, 24H, -CH₂(CH₂)₂CH₃), 1.25 (m, 16H, -CH₂CH₂CH₂-CH₃), 1.60 (m, 16H, -CH₂CH₂CH₂CH₃), 4.22 (t, 16H, -CO₂-CH₂-), 5.18 (s, 16H 1-methylene), 10.30 (s, 4H, methine); UV (CHCl₃), λ_{max} (nm) 475, 523, 580, 637; IR (KBr), ν (cm⁻¹) 3410 (s, NH), 2960-2850 (s, CH), 1738 (s, C=O); Calcd for C₆₈H₈₄O₁₆N₄ (MW 1223), C 66.75, H 7.74, O 20.92, N 4.58, Found: C 66.84, H 7.58, O 21.02, N 4.60.
11. Physical, spectral and elemental analysis data of P4H-Cl: mp. 200°C; ¹H NMR (CDCl₃), δ (ppm) -3.56 (b, 2H, NH), 1.82 (m, 32H, -CH₂(CH₂)₂CH₂Cl), 3.59 (t, 16H, -(CH₂)₃CH₂-Cl), 4.11 (t, 16H, -CO₂CH₂-), 5.16 (s, 16H, 1-methylene), 10.31 (s, 4H, methine); UV (CHCl₃), λ_{max}(nm) 468, 525, 578, 635; IR (KBr), ν (cm⁻¹) 3412 (s, NH), 2962-2854 (s, CH), 1736(s, C=O); Calcd for C₆₈H₈₆O₁₆N₄Cl₈ (MW 1450), C 54.49, H 5.78, O 17.07, N 3.74, Cl 18.92, Found C 54.58, H 5.72, O 17.12, N 3.70, Cl 18.94.
12. Dolpin, D. *The Porphyrins*; Academic Press: New York, U. S. A., 1978; Vol. I-VI.
13. X-ray diffraction experiments were performed with JEOL JDX using CuKα radiation at 40 KV×15 mA. Since the quantity of the sample was small, the sample was sealed in a fine glass capillary to be irradiated by X-ray, and the capillary was set in the middle of the furnace. The incident X-ray was collimated with a pin-hol slit, and the diffraction pattern were recorded on high sensitive Kodak DEF-5 film so as to minimize the exposure time.
14. For electron microscopy, the specimen was solved in ethanol-chloroform mixture (3 : 1) and a drop of the solution was spread on a thin amorphous carbon film fixed beforehand on an electron microscopic grid. After evaporating the solution in air, the structural changes of the specimens were examined with JEOL 2000-FX equipped with a high temperature specimen holder.

A Simple Flow Method to Study Photochemistry of Molecules Adsorbed on Ag Colloid Surface

Jung Sang Suh*, Nak Han Jang, and Dae Hong Jeong

Department of Chemistry Education,
Seoul National University, Seoul 151-742, Korea

Received July 29, 1994

Enhanced surface photochemistry of molecules adsorbed on surfaces capable of producing surface-enhanced Raman has been known.¹⁻⁴ Photochemistry at surfaces may be enhanced by the same field enhancement responsible for surface-enhanced Raman scattering (SERS).

SERS spectroscopy in principle provides a powerful means for the study of surface chemical reactions, because these reactions directly results in the changes in SERS spectra of adsorbed molecules.^{5,6}

Recently, Suh *et al.* have studied the kinetics of the photodecomposition of 2-pyrazinecarboxylic acid adsorbed on silver colloid surfaces using SERS as a probe.⁷ They have used a capillary as the sample cell to increase the effect of irradiation. Both photochemistry and surface-enhanced Raman were monitored by focused Ar ion laser light traversing the capillary containing a sample solution, without flowing. In this case, it is possible to use SERS as a probe because the rate of the photodecomposition is relatively slow. If the rate of photochemical decomposition of a molecule adsorbed on silver colloid surfaces is relatively fast, it is almost impossible to use SERS as a probe to study the kinetics of photochemistry since SERS signal should be accumulated for a certain period to obtain reasonable signal-to-noise ratios. For a fast photochemistry, the accumulation time of Raman signal to get reasonable signal-to-noise ratio may be much longer than its photochemical reaction time.

In this communication, we report that the flow method designed to investigate the relatively fast photochemical reactions of molecules adsorbed on Ag colloid surfaces using SERS as a probe.

The schematic diagram of the flow system used is shown in Figure 1. The flow cell was a modified graduated cylinder. A stop cock was attached to the cut-out bottom of the graduated cylinder. A standard 1.5-1.8 mm Pyrex capillary tube was used as a Raman cell. To make the flow of the sample solution smooth, the tip of the outlet was dipped in a water solution whose water level was kept constant.

The driving force for the flow is the pressure difference between the outlet and the top of solution in the flow cell. Therefore, the flow rate can be written as⁸

$$F = -A_{gc} \frac{dh}{dt} = c\rho gh$$

where A_{gc} is the cell cross sectional area, h the height of solution with time, ρ the density, g the gravitational constant, and c a constant. Solving this differential equation gives the height of solution with time as

$$h = h_0 \exp(-t/\tau_0)$$

where h_0 is the height of solution at $t=0$ and $\tau_0 = A_{gc}/c\rho g$